This article has been accepted for publication in a future issue of this journal, but has not been fully edited. Content may change prior to final publication. Citation information: DOI 10.1109/TSM.2019.2907790, IEEE Transactions on Semiconductor Manufacturing

Marker Layout for Optimizing the Overlay Alignment in a Photolithography Process

Ki Bum Lee and Chang Ouk Kim

***Abstract*—In the photolithography process of wafer fabrication, a mask pattern is transferred to a wafer in a layer-by-layer fashion, and the pattern alignment of adjacent layers is critical to the wafer yield. To enhance the alignment precision, an overlay metrology system measures the overlay error at some markers on the wafer, and the error information is used for constructing an overlay correction model. During the overlay alignment, the layout of the markers has a significant impact on the correction of the overlay error. After the maximum number of available markers has been determined based on the quality and turn-around time of the target device, the positions of those markers should be determined in such a way that the overlay error correction model shows robust performance for future wafers. In this study, we propose a sparse particle swarm optimization algorithm to find an optimal marker layout in terms of robust performance characterized by the overlay error prediction and irregularity of marker positions. In the experiment, the performance of the marker layouts suggested by several search algorithms was tested on three different layers, and the proposed algorithm demonstrated superiority over the other algorithms.**

***Index Terms*—Photolithography process, overlay sampling, marker layout, sparse particle swarm optimization, overlay error, irregularity of marker position.**

I. Introduction

IN SEMICONDUCTOR manufacturing, the wafer fabrication process consists of a series of operations, such as photolithography, deposition, etching, and polishing. During these operations, integrated circuits are fabricated by successively stacking patterned layers of different materials on a wafer. When depositing the next layer onto the wafer, the pattern in the layer should be accurately aligned with other patterns in the preceding layers to ensure that integrated circuits can function properly [1]. Photolithography is the process of transferring geometric patterns on a mask (also referred to as a reticle) to the surface of the wafer, and this process affects the alignment of patterns between adjacent layers. To enhance the alignment precision in the photolithography process, an overlay metrology system measures the relative positions of the markers on the wafer, and the metrology results are used to construct a statistical correction model for overlay control.

Overlay error is considered one of the key factors affecting the yield of the semiconductor product because this error represents the displacement between the current exposure layer and the preceding layer [2]. At some points on the wafer, the metrology system measures overlay errors that are the differences between the points in the current layer and the corresponding points in the next mask pattern. The point at which an error is measured is called a marker, and the overlay control performance depends on the marker layout: the number and sampling plan of markers in an exposure field of a wafer. Here, the sampling plan means the distribution of markers. Generally, overlay control is more accurate when more markers are allocated on the field. However, the turn-around time (TAT) of a photolithography process becomes longer (bottleneck process) as the number of markers increases. Thus, the number of markers is limited in an actual photolithography process and is mostly determined by the expert's experience, taking into account the TAT, preliminary experimental data, and process conditions.

Related literature has proposed several overlay sampling strategies. Rangarajan *et al.* [3] designed several 25-marker layouts on a wafer and indicated that the type of marker layout can have a substantial effect on the overlay control. Chien *et al.* [4] introduced a Hyper-Graeco-Latin square design into a marker layout, seeking to elicit more overlay error information related to translation, magnification and rotation. Chue *et al.* [5] proposed several nine-marker layouts for a 5×5 marker array within an exposure field of a wafer according to two guidelines for determining the optimal marker layout: symmetry in x and y coordinates and spatial coverage. These early studies obtained the optimal marker layout based on expert knowledge and heuristic reasoning. However, this approach is difficult to apply to a work-site process as the minimum number of markers for overlay quality requirements increases from tens to hundreds. Therefore, rule-based sampling methods have been preferred as an alternative. Aung *et al.* [6] suggested an automated rule-based sparse sampling method that considers the homogeneity and uniformity of marker distribution to capture the overlay variation across the wafer. Subramany *et al.* [7] devised a criterion for test balancing, scan direction balancing and field balancing of markers and utilized these balancing rules to generate a marker layout that can achieve maximum spatial uniformity.

To the best of our knowledge, this study is the first to

This research was supported in part by the National Research Foundation of Korea (NRF) grant funded by the Ministry of Education (NRF-2015H1A2A1031081-Global Ph.D. Fellowship Program), by an NRF grant funded by the Ministry of Science and ICT (NRF-2016R1A2B4008337), by the Graduate School of YONSEI University Research Scholarship Grants in 2018, and by SK Hynix Co., Ltd.

The authors are affiliated with the Department of Industrial Engineering, Yonsei University, Seoul 03722, Republic of Korea (e-mail: kimco@yonsei.ac.kr).

This article has been accepted for publication in a future issue of this journal, but has not been fully edited. Content may change prior to final publication. Citation information: DOI 10.1109/TSM.2019.2907790, IEEE Transactions on Semiconductor Manufacturing

investigate whether a metaheuristic-based optimization approach is effective at improving the quality of a marker layout. Rule-based approaches create coordinates of markers by combining random sampling and some heuristic rules, and these approaches aim to distribute markers evenly across the entire wafer. Although there are a number of feasible marker layouts that satisfy the rules, rule-based approaches determine the final marker layout in a random fashion, which makes it difficult to ensure reliable performance. In contrast, the metaheuristic approach can find an optimal marker layout that shows robust performance for future wafers in terms of overlay error prediction if the approach minimizes the total predicted overlay error of experimental wafers and the irregularity (nonuniformity) of marker positions. In particular, the spatial distribution of markers is an important variable for achieving robust performance because of wafer-to-wafer irregularity in the overlay pattern. A marker layout optimizing the total overlay alignment of experimental wafers is likely to be overfitted—marker positions will be determined biased toward the overlay patterns of the experimental wafers. The overfitted layout is not generally optimal for future wafers, resulting in a large total overlay misalignment in the actual production stage. Therefore, photolithography engineers seek a layout that achieves a low predicted overlay error among the layouts in which markers are evenly distributed in the field of the wafer or in the entire wafer.

In this study, particle swarm optimization (PSO), a popular metaheuristic in the semiconductor manufacturing field [8], [9], is tailored to generate overlay sampling plans in a data-driven manner. The proposed sparse particle swarm optimization (SPSO) algorithm suggests potential solutions in consideration of the sparsity of markers, and thereby, the search focuses on both error correction performance and uniformity of the marker positions. In a performance test, the proposed algorithm succeeded in finding a better marker layout than other conventional heuristic and metaheuristic methods.

The remainder of this paper is organized as follows. Section II introduces the principles of PSO and SPSO algorithms and their application in the overlay sampling problem. Section III presents the procedure for choosing the optimal number of markers and evaluates the quality of marker layouts suggested by the SPSO and other competitive algorithms. Finally, conclusions and future research topics are discussed in Section IV.

II. Proposed Method

A. Principle of PSO

PSO is a population-based metaheuristic that emulates a swarm of flocking birds [10]. This algorithm has been widely applied to many optimization problems in manufacturing fields due to its simple implementation and outstanding performance. In PSO, the swarm searches promising regions in the solution space. Specifically, each particle in the swarm represents a potential solution and performs a stochastic search, moving to a new potential solution from iteration to iteration based on the following equations:

$$\boldsymbol{X}_k^{t+1} = \boldsymbol{X}_k^t + \boldsymbol{V}_k^t, \tag{1}$$

$$\boldsymbol{V}_k^t = w\boldsymbol{V}_k^{t-1} + c_1 r_1(\boldsymbol{p}_k^t - \boldsymbol{X}_k^t) + c_2 r_2\left(\boldsymbol{p}_g^t - \boldsymbol{X}_k^t\right), \tag{2}$$

where $\boldsymbol{X}_k^t$ denotes the position of particle k at iteration t and $\boldsymbol{V}_k^t$ is the velocity indicating the direction of the particle for the next iteration. In addition, w is an inertia factor; c_1 and c_2 are two positive constants called the cognitive and social learning rates, respectively; and r_1 and r_2 are uniformly distributed random numbers in the range of [0, 1]. At each iteration, the velocity of each particle $\boldsymbol{V}_k^t$ is updated based on its velocity in the previous iteration $\boldsymbol{V}_k^{t-1}$, the local best particle (local solution) $\boldsymbol{p}_k^t$, and the global best particle (global solution) $\boldsymbol{p}_g^t$. $\boldsymbol{p}_k^t$ is the best solution of particle k from its own experience. The experience means the fitness values of potential solutions that a particle has found so far. $\boldsymbol{p}_g^t$ is the best solution of all particles from global experience, which attracts the other particles to move toward itself, helping them search for a more plausible space. When the velocities and particles are updated as specified in Eqs. (1) and (2), the performance of each particle is evaluated using a fitness function. This procedure is repeated until the PSO iteration t reaches the maximum iteration T. Then, PSO selects the final $\boldsymbol{p}_g^T$ value as the optimal solution.

In the PSO algorithm, w is a critical parameter for controlling the speed and search direction of the particle swarm [11]. A large value of w increases the global exploration of the swarm, keeping each particle at its own pace and direction. In contrast, a small value of w increases the local exploration of the swarm, making each particle converge quickly to the local minima as greatly influenced by the local best and global best particles. To balance global exploration and local exploration, we suggest changing the w value dynamically, as presented in Eq. (3), during the PSO search.

$$w = w_{max} - \frac{w_{max} - w_{min}}{iteration_{max}} \times iteration. \tag{3}$$

This equation makes w linearly decrease from w_{max} to w_{min}, and this decrease leads to the velocity of the particles gradually decreasing as the number of iterations increases. Therefore, the swarm actively explores the solution space in the early stage of the search and exploits only the most promising areas in the last stage of the search.

B. PSO for the overlay sampling problem

Overlay sampling is a combinatorial optimization problem where only M critical markers are selected among all N feasible markers (M<N), which can maximize the performance of the overlay correction model. In PSO for overlay sampling, each particle represents a potential solution (marker layout) of an N-dimensional vector, $\boldsymbol{X} = (x_1, x_2, \dots, x_N)$, where each element x_i $(i = 1, \dots, N)$ is a real number. Each element should have a value of one or zero to indicate that the corresponding marker is selected, and a marker layout has M elements of value one to represent M markers. At each PSO iteration, we can assign each element a probability value in [0, 1] by transforming the original PSO solution x_i into the

This article has been accepted for publication in a future issue of this journal, but has not been fully edited. Content may change prior to final publication. Citation information: DOI 10.1109/TSM.2019.2907790, IEEE Transactions on Semiconductor Manufacturing

logistic function value p_i [12] as follows:

$$p_i = \frac{1}{1+\exp(-x_i)}, where \;\; 1 \le i \le N. \quad (4)$$

Then, a feasible marker layout can be obtained by the probabilistic selection of M markers using the distribution defined in Eq. (4). The higher the probability of a marker is, the greater the contribution of the marker to the fitness function of the overlay sampling problem. However, there is a chance that the probabilistic choice does not select a marker with a high contribution. This property makes the PSO explore the solution space and escape from local minima. Therefore, it is reasonable to use the probabilistic selection rule. According to Poli *et al.* [12] and Agrafiotis and Cedeno [13], probabilistic choice can be applied either to the velocity or to the solution. Both methods strengthen the exploration of the solution space.

C. SPSO for the overlay sampling problem

SPSO differs from PSO for overlay sampling in that SPSO updates the marker probability distribution in consideration of the distance information between markers. It is assumed that we have a probability distribution of markers at each PSO iteration. Then, SPSO selects only one marker at a time and selects the first marker in the same way as PSO for overlay sampling—the first marker is selected using the distribution presented in Eq. (4). For the selection of the second or a subsequent marker, however, the probability distribution of the remaining markers depends on the selected markers as follows in Eq. (5):

$$\tilde{p}_i = \frac{e^{d_i p_i} - 1}{\sum_{i=1}^{N}\left(e^{d_i p_i} - 1\right)}. \quad (5)$$

In this equation, $\tilde{p}_i$ is the selection probability of the i-th remaining marker calculated by the softmax function with weight d_i, which is the minimum of the distances between the i-th remaining marker and the selected markers. A larger value of d_i means that the i-th marker is located far from the selected markers. Therefore, if a marker with a large value of d_i is selected, the marker layout can measure the overlay error of the new wafer area. The softmax function amplifies the original selection probability p_i $(i = 1, \dots, N)$ in Eq. (4) by considering the minimum distance d_i. The larger the value of d_i is, the higher the chance the element has to be selected. This characteristic allows SPSO to generate more promising potential solutions, taking into account the sparsity of the markers. Although most softmax functions adopt the form $e^x / \sum e^x$, SPSO adds -1 to the exponent term to make already selected markers have a selection probability of zero. The procedure of the SPSO is described as follows.

Procedure 1 SPSO for the overlay sampling problem

Step 1) Initialize K particles randomly in [0, 1], and set $t = 1$.
Step 2) Obtain K potential solutions by repeating the following substeps for each particle.
  2.1. Transform each element x_i of the particle into probability p_i using Eq. (4).
  2.2. Select the first marker based on the probability distribution.
  2.3. For each remaining marker, calculate the minimum distance to the selected marker(s).
  2.4. Update the probability $\tilde{p}_i$ of the remaining markers using Eq. (5).
  2.5. Select the next marker based on the updated probability distribution.
  2.6. Repeat steps 2.3 – 2.5 until M markers are selected. Set the layout of the selected M markers as the potential solution of the particle at iteration t.
Step 3) Obtain the fitness values of potential solutions.
Step 4) For each particle, renew its local best $\boldsymbol{p}_k^t$ if the solution is the best in its experience.
Step 5) Find the best solution of all particles and update the global best $\boldsymbol{p}_g^t$.
Step 6) Change the iteration number t to $t+1$.
Step 7) Update the velocities and positions of all particles using Eqs. (1) and (2).
Step 8) Repeat steps 2 – 7 until t reaches T.
Step 9) Output the global best $\boldsymbol{p}_g^T$ as the final solution.

III. Experiment

The overlay measurement data used in the experiments were collected from the photolithography equipment of a Korean semiconductor company in 2017. These data included a total of 118 wafers (two wafers per lot) from three different layers: Layer A contained 40 wafers and 124 markers per field, layer B contained 38 wafers and 115 markers per field, and layer C contained 40 wafers and 121 markers per field. Each wafer had up to 118 fields with evenly spaced markers in a 2×1 marker array, and each of the markers had position information and overlay error measurements. For each layer, two-thirds of the wafer data were used to search for the optimal marker layout (experimental data), and the rest of the data were used for the performance test of the marker layout (test data). Given a marker layout, the intrafield high-order process correction (iHOPC) model [14] was trained using the overlay errors measured at the markers to correct the overlay error during the experiments. The photolithography tool used in the experiment supports only the iHOPC model. More complex models, such as support vector regression, artificial neural networks, and random forests, may show higher performance than iHOPC, but the tool does not currently support these models. As a result, it is not possible to measure the performance of the complex models.

The marker layout optimization consisted of two phases. The first phase was to determine the number of markers used in a field among the total feasible markers. Although the number of total feasible markers in a field varied from layer to layer, the number of sampled markers remained the same to maintain a consistent TAT for the entire process. The second phase was to determine the location of the markers. If the sampling number of markers is fixed, the determination of the marker layout can be regarded as a combinational optimization problem. Therefore, we applied several metaheuristic algorithms to

This article has been accepted for publication in a future issue of this journal, but has not been fully edited. Content may change prior to final publication. Citation information: DOI 10.1109/TSM.2019.2907790, IEEE Transactions on Semiconductor Manufacturing

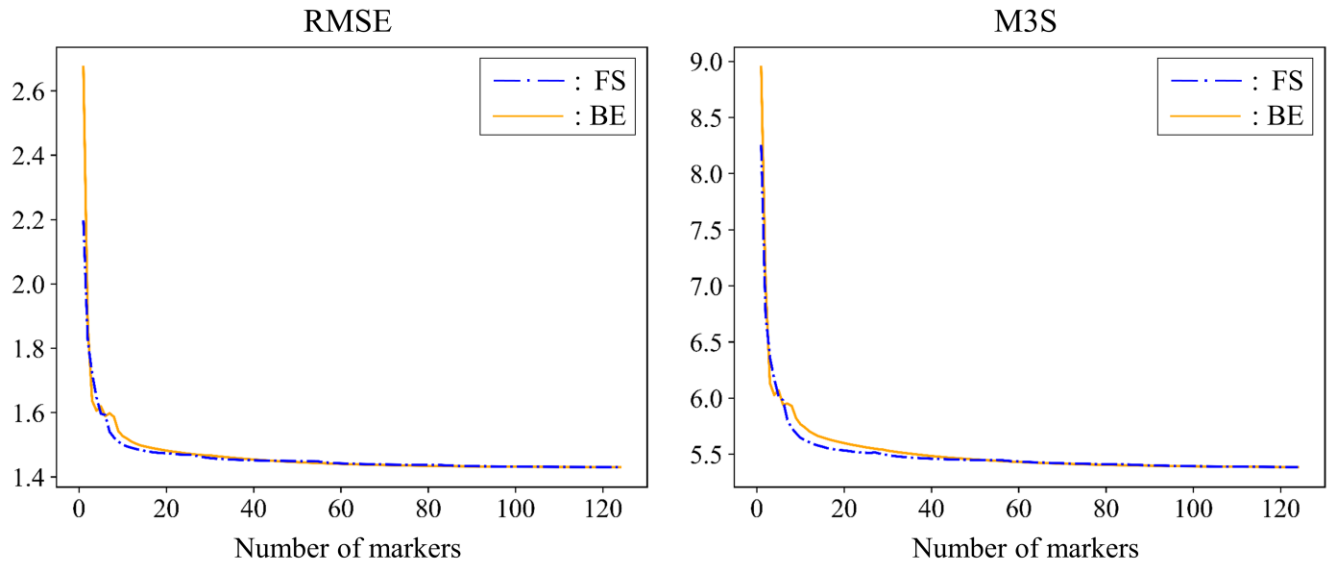

Fig. 1. Performance changes of forward selection (FS) and backward elimination (BS) algorithms with respect to the number of markers.

search for the optimal marker layout for each layer and quantitatively compared the layouts in terms of the fitness function.

A. *Performance measures of sampling efficiency*

To evaluate the efficiencies of the marker layouts, the root mean squared error (RMSE) and mean+3 sigma (M3S) were adopted as performance measures. These measures were calculated with respect to the overlay residual between the actual overlay and prediction (correction) model at each feasible marker position. The measures are defined as follows:

$$y_i^{res} = y_i - \hat{y}_i, \tag{6}$$

$$\text{RMSE} = \sqrt{\frac{1}{n}\sum_{i=1}^{n}(y_i^{res})^2}, \tag{7}$$

$$\text{M3S} = Mean(y^{res}) + 3\sigma(y^{res}). \tag{8}$$

Here, y_i is the actual overlay value (overlay error) evaluated at marker i, $\hat{y}_i$ is the prediction value at the marker, y_i^{res} is the overlay residual, n is the total number of overlay markers in a wafer, and $Mean(y^{res})$ and $\sigma(y^{res})$ are the average and standard deviation, respectively, of the overlay residuals. The more accurately that the overlay correction model predicts the actual value, the lower the values of RMSE and M3S become. In addition, a sampling accuracy indicator (SAI) [5] is adopted that normalizes the RMSE and M3S to consider the different scales of RMSE and M3S. This indicator is defined as

$$SAI(M) = 1 - \frac{\left|M_{selected} - M_{full\ sampling}\right|}{M_{full\ sampling}}, \tag{9}$$

where $M_{selected}$ and $M_{full\ sampling}$ are measures of the overlay error (i.e., RMSE or M3S) from the selected and full sampling schemes, respectively. In general, as the sampling number of markers increases, the performance of the layout improves. $M_{full\ sampling}$ represents the best performance, that is, the ideal value of a measure when all feasible markers are used, and $M_{selected}$ represents the current value of a measure when only the selected markers are used. The SAI indicates the degree to which $M_{selected}$ approximates $M_{full\ sampling}$; as $M_{selected}$ approaches $M_{full\ sampling}$, the SAI value approaches 1.

B. *Determination of the optimum number of markers in a field*

According to the field engineers' requirements, the sampling number of markers available in a field was limited. This lower limit was due to the quality of the overlay control, and the upper limit was due to the TAT of the photolithography process. If the number of markers was too small, the amount of overlay error information might not be sufficient to construct the overlay correction model. Then, this effect would reduce the robustness of the correction model parameters, leading to a reliability issue for the entire photolithography process. In addition, as the number of markers increased, the measurement time became longer, and this effect decreased the productivity of the process.

In the case of the target product line, the lower and upper limits of the number of markers were 10 and 30. Within the limits, the number of markers is commonly decided through expert consultation. In this study, however, the relationship between the number of markers and the overlay control quality was investigated, and the optimal number of markers was obtained from the results. During the experiment, we used forward selection (FS) and backward elimination (BE) searches to check the performance of the overlay correction model with

This article has been accepted for publication in a future issue of this journal, but has not been fully edited. Content may change prior to final publication. Citation information: DOI 10.1109/TSM.2019.2907790, IEEE Transactions on Semiconductor Manufacturing

TABLE I
SAI PERFORMANCE FOR DIFFERENT SAMPLING NUMBERS OF MARKERS

Number of markers	Layer A				Layer B				Layer C			
	SAI(RMSE)		SAI(M3S)		SAI(RMSE)		SAI(M3S)		SAI(RMSE)		SAI(M3S)	
	FS	BE	FS	BE	FS	BE	FS	BE	FS	BE	FS	BE
1	46.4%	13.1%	46.7%	33.8%	-30.8%	-49.3%	-14.2%	-23.0%	-181%	-237%	-146%	-165%
10	95.1%	93.3%	95.2%	92.9%	91.4%	89.8%	91.5%	89.7%	92.8%	95.5%	93.3%	95.7%
15	96.5%	95.5%	96.6%	95.1%	93.9%	92.8%	94.3%	93.2%	95.8%	96.8%	96.1%	96.9%
18	**96.9%**	96.1%	**97.1%**	95.7%	**94.8%**	93.9%	**95.1%**	94.3%	96.3%	**97.1%**	96.6%	**97.2%**
20	**97.0%**	96.4%	**97.3%**	96.0%	**95.5%**	94.7%	**95.7%**	94.9%	96.5%	**97.2%**	96.8%	**97.6%**
25	97.3%	97.1%	97.6%	96.7%	96.3%	96.2%	96.6%	96.3%	96.7%	97.8%	97.1%	98.1%
30	98.0%	97.5%	98.0%	97.3%	96.8%	97.2%	97.2%	97.2%	98.2%	98.3%	98.2%	98.5%
100	99.9%	99.9%	99.9%	99.9%	99.2%	99.9%	99.3%	99.9%	99.9%	99.9%	99.9%	99.9%
Full	1.431		5.385		3.638		13.629		2.659		10.053	

respect to the sampling number of markers in a wafer field. FS starts with an empty set solution and picks the best marker one at a time until all markers are included. Here, the best marker means a marker that shows the highest improvement in fitness defined in Eq. (10) when added to the solution. BE starts with a universal set solution (which includes all markers) and removes the most unimportant marker that shows the least impact on the fitness one at a time until the solution reaches an empty set. Both approaches can produce approximately optimal solutions for all possible numbers of markers in a fast and efficient way.

The results of FS and BE searches for layer A are presented in Fig. 1. Both the RMSE and M3S of the overlay correction model sharply decreased until 10 markers were used, and then the decreasing rate gradually reduced. In addition, the graphs of the RMSE and M3S monotonically decreased. These results proved that at least 10 markers should be used to obtain robust model parameters, and it is ideal to use all feasible markers to maximize the performance of the overlay correction model.

When the search processes were performed to individually minimize the RMSE and M3S, the resulting solutions were optimized for each fitness function. If the selected markers were the same in both searches, they could be directly implemented on the equipment as the final marker layout. If not, additional steps were required to suggest a single solution that considered both the RMSE and M3S. Therefore, we combined the above RMSE and M3S measures into a single fitness function as follows:

$$Fitness = \alpha \times SAI(RMSE) + \beta \times SAI(M3S), \qquad (10)$$

where the fitness function consisted of the RMSE and M3S measures scaled by the SAI. Then, α and β were set to 0.5 because the RMSE and M3S have the same importance in the overlay control.

Table 1 represents the SAI performance results of the FS and BE searches for layers A, B, and C by using the fitness function defined in Eq. (10). For each layer, the RMSE and M3S were expressed as a percentage of the SAI in Table 1, and a value of 100% indicates the full marker model. The last row in the table indicates the actual RMSE and M3S values of the full marker model using all the overlay information. When using only a single marker, negative values appeared in layers B and C, and these values denoted overlay errors that were exacerbated by the incomplete model. As the number of markers increased, layers A and C showed similar performance improvements with values of approximately 95% with 10 markers, 97% with 20 markers, and 98% with 30 markers. In contrast, layer B recorded values of 91% with 10 markers, 95% with 20 markers, and 97% with 30 markers, showing slightly larger overlay errors than the other layers. Since the performance differed according to the layer type, the worst layer should be chosen as a criterion for the minimum quality of the overall photolithography process. Therefore, the number of markers ensuring approximately 95% performance was determined to be 18 based on the layer B results. Although the 20-marker layout improved the performance of layer B slightly more, this layout was not efficient from the viewpoints of the TAT and the other layers.

C. Experimental results of marker layout

In this section, we compared the quality of the marker layouts found by SPSO and other search algorithms: the baseline algorithm, FS, BE, genetic algorithm (GA), and PSO. FS and BE were conducted in the same manner as in the previous experiment. The baseline algorithm designed a marker layout by considering the spatial symmetry and uniformity of markers, which are common properties of heuristic reasoning suggested in rule-based studies. We evaluated the performance of several potential baselines and selected a marker layout with the best average performance as the baseline. The baseline rules are introduced later in this section. The parameters of the GA were chosen as follows: the population size was 100, the number of iterations was 300, the crossover rate was 80%, and the mutation rate was 3% [15]. For the PSO and SPSO algorithms, the parameters were chosen as follows: the population size was 100, the number of iterations was 300, w_{max} and w_{min} were 0.9 and 0.4, respectively, and c_1 and c_2 had values of 2 [12]. Moreover, an irregularity measure was used to calculate the average minimum distance between the total feasible

This article has been accepted for publication in a future issue of this journal, but has not been fully edited. Content may change prior to final publication. Citation information: DOI 10.1109/TSM.2019.2907790, IEEE Transactions on Semiconductor Manufacturing

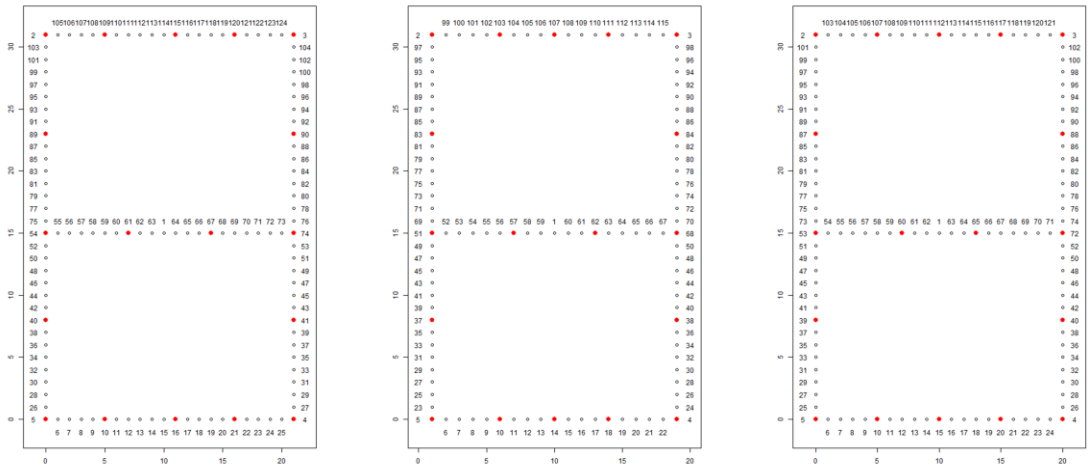

Fig. 2. Baseline layouts for layers A (left), B (middle) and C (right).

TABLE II
PERFORMANCE TEST OF OVERLAY ALIGNMENT SCENARIOS ($\alpha = \beta = 0.45,\ \gamma = 0.1$)

Layer	Algorithm	RMSE X	RMSE Y	M3S X	M3S Y	RMSE ratio	M3S ratio	Irregularity	Fitness
A	Baseline	0.718	0.744	2.706	2.813	-	-	4.736	96.37%
	SPSO	0.711	0.742	2.679	2.775	0.52%	1.17%	4.660	97.16%
	FS	0.713	0.741	2.684	2.772	0.51%	1.13%	6.009	94.45%
	BE	0.722	0.744	2.720	2.800	-0.35%	-0.02%	5.160	95.30%
	GA	0.722	0.747	2.724	2.813	-0.54%	-0.32%	6.000	93.29%
	PSO	0.716	0.741	2.695	2.792	0.33%	0.56%	6.311	93.46%
B	Baseline	1.898	2.271	7.134	8.535	-	-	4.546	94.80%
	SPSO	1.887	2.245	7.028	8.421	0.88%	1.40%	4.763	95.41%
	FS	1.895	2.224	7.038	8.341	1.20%	1.85%	10.742	86.25%
	BE	1.906	2.281	7.137	8.549	-0.43%	-0.11%	5.082	93.36%
	GA	1.922	2.298	7.094	8.655	-1.22%	-0.51%	4.814	93.39%
	PSO	1.896	2.311	7.068	8.649	-0.90%	-0.31%	5.113	92.98%
C	Baseline	1.330	1.387	5.034	5.226	-	-	4.612	96.06%
	SPSO	1.311	1.363	4.944	5.139	1.60%	1.72%	4.825	97.15%
	FS	1.332	1.384	4.981	5.224	0.06%	0.54%	7.612	89.83%
	BE	1.335	1.353	5.016	5.111	1.09%	1.29%	5.049	96.23%
	GA	1.334	1.385	5.030	5.216	-0.05%	0.13%	6.369	92.29%
	PSO	1.335	1.387	4.994	5.225	-0.16%	0.41%	5.650	93.92%

markers and the selected markers as follows:

$$Irregularity = \frac{1}{n}\sum_{i=1}^{n}\left(dist(l_i, n\_l_i)\right)^2, \qquad (11)$$

where l_i is a marker location (i = $1, \ldots, n$) and n_l_i indicates the location of its nearest neighboring marker in the selected marker set. The irregularity measures the degree to which the selected markers in a layout were evenly distributed to efficiently extract the overall overlay error of each wafer. If the markers were spread evenly throughout the field, the irregularity value would be low, but if some markers were densely located in a certain field area, this value would become high. A high level of irregularity in a marker layout indicated that the layout might have risks of overfitting to the current data and showing unstable performance when implemented in the actual production stage. To give a penalty to such marker layouts, the irregularity measure was included in the fitness function defined in Eq. (12), where α, β, and γ are the weights of the fitness components and satisfy $\alpha + \beta + \gamma = 1$.

$$Fitness = \alpha \times SAI(RMSE) + \beta \times SAI(M3S) + \gamma \times SAI(irregularity) \qquad (12)$$

The baseline layouts for layers A, B and C are shown in Fig. 2. For each layer, the number of total feasible markers varied from 115 to 124, and the positions of these markers were

This article has been accepted for publication in a future issue of this journal, but has not been fully edited. Content may change prior to final publication. Citation information: DOI 10.1109/TSM.2019.2907790, IEEE Transactions on Semiconductor Manufacturing

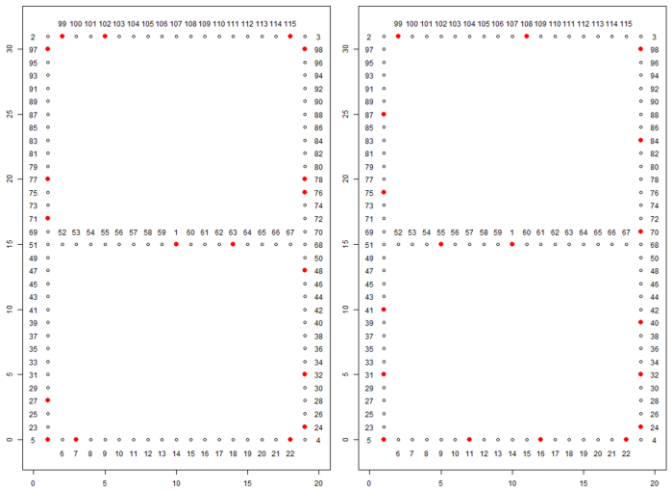

Fig. 3. Optimal marker layouts found by the FS (left) and SPSO (right) algorithms.

slightly different. Considering the densities of the markers, the baseline layouts were determined according to the following rules. First, six markers at each corner were selected. Then, five markers were arranged at equal intervals on both the vertical axis and the outer horizontal axis. Finally, the remaining two markers were placed on the centerline. The irregularity values of the baseline layouts were 4.736 for layer A, 4.546 for layer B, and 4.612 for layer C, and these values replaced those of $M_{full\ sampling}$ in the calculation of the SAI(irregularity) performance defined in Eq. (9).

The search algorithms were applied to the experimental dataset of each layer and determined the final layouts with the highest fitness values. During this experiment, the weights α, β and γ of the fitness function were set to 0.45, 0.45, and 0.1, respectively. Table 2 shows the detailed test performance of the marker layouts found by the algorithms. The X and Y terms written after RMSE and M3S represent the overlay residuals measured along the x-axis and y-axis, respectively. The RMSE ratio and the M3S ratio indicate the improvement in performance of the marker layouts compared to that of the baseline layout. The fitness is an integrated measure in Eq. (12) that includes the RMSE, M3S, and irregularity. In this experiment, SPSO demonstrated its superiority over the other search algorithms. The SPSO layouts recorded fitness values of 97.16% for layer A, 95.41% for layer B, and 97.15% for layer C, which were the highest values among the layouts. The FS layouts obtained positive RMSE and M3S ratios with a high level of irregularity in all layers, implying high overfitting risk. Only the BE layouts achieved better overlay control performance than the baseline for layer C. The PSO and GA layouts did not record any significant performance improvements. This finding meant that it was difficult to find outstanding marker layouts by simply introducing a metaheuristic algorithm to generate marker layouts. To generate ideal solutions, the search algorithm should be tailored to suit the purpose of the given problem, such as the approach of SPSO.

Fig. 3 illustrates the final solutions for layer B proposed by the FS and SPSO algorithms. In the FS layout, nine markers (5, 7, 22, 24, 27, 97, 98, 99, and 115) were located at the corners, so the spacing between the markers was relatively wide and irregular. In particular, there was no marker in the middle of the outer horizontal axis (region [8, 21] and region [103, 114]). In this case, even if the FS layout was effective for the given experiment data, this layout would be uncertain to cope well with new wafers whose overlay errors were largely formed in such regions in an actual manufacturing process. In contrast, of the nine corner markers in the FS layout, the SPSO layout contained only a subset of those corner markers (5, 22, 24, 98, 99), and the remaining selected markers were evenly distributed, maintaining adequate space throughout the field. Due to its low irregularity, it was expected that the SPSO layout would exhibit reliable error control when new wafers have irregular overlay errors in any region. Therefore, we concluded that it would be desirable to introduce the SPSO layouts that achieved low irregularity and excellent overlay control performance on the test wafers because the experimental data could not reflect all exceptional cases that might occur in an actual manufacturing process.

We conducted an additional experiment to test the robustness of the search algorithms against different fitness functions. Table 3 summarizes the average test results for marker layouts in layers A, B, and C, where the ratio of γ in the fitness function was gradually increased from 0.01 to 0.2. As the ratio of γ increased, the importance of irregularity became a primary factor in the layout quality assessment; however, the performance in RMSE and M3S deteriorated to some extent. Specifically, when γ was 0.01, all marker layouts seemed to have similar fitness of 95% or more. That is, if we did not consider irregularity as an important factor, the advantage of the SPSO layout was not remarkable. As the value of γ gradually increased, however, the gap between the fitness values of the SPSO layout and the other layouts gradually increased. The FS layout recorded higher SAI(RMSE) and SAI(M3S) values than the baseline layout in all experiments but showed the lowest irregularity in all test experiments. Consequently, the fitness of the FS layouts decreased the most among the layouts. The BE layout was the second best but was lower than the SPSO layout in all performance measures. The standard PSO and GA algorithms exhibited acceptable quality compared to SPSO at low values of γ, but the fitness of the layouts of these algorithms gradually decreased as γ increased. Finally, the SPSO layout achieved the best fitness in all test experiments regardless of the ratio of γ. Moreover, when the value of γ was greater than 0.15, the SPSO layout showed better quality than the baseline layout in all performance measures: the SAI(RMSE), SAI(M3S), and SAI(irregularity). In particular, it was noteworthy that the SPSO layout achieved 100% SAI(irregularity)—SPSO was better than the baseline with respect to the irregularity. The SAI(irregularity) was calculated based on the irregularity of the baseline, where markers were selected to minimize the irregularity by the heuristic rules of the field engineers. Therefore, it was difficult for the standard search algorithms to

This article has been accepted for publication in a future issue of this journal, but has not been fully edited. Content may change prior to final publication. Citation information: DOI 10.1109/TSM.2019.2907790, IEEE Transactions on Semiconductor Manufacturing

TABLE III
PERFORMANCE TEST OF OVERLAY ALIGNMENT SCENARIOS

$\gamma = 0.01$ $(\alpha = \beta = 0.495)$				
Layout	SAI(RMSE)	SAI(M3S)	SAI(irregularity)	Fitness
Baseline	95.35%	95.19%	100%	95.32%
SPSO	**96.33%**	**96.54%**	**97.08%**	**96.44%**
FS	**96.07%**	**96.50%**	31.57%	95.64%
BE	95.66%	95.65%	65.82%	95.36%
GA	95.77%	95.90%	53.26%	95.41%
PSO	95.90%	96.36%	46.57%	95.64%
$\gamma = 0.05$ $(\alpha = \beta = 0.475)$				
Layout	SAI(RMSE)	SAI(M3S)	SAI(irregularity)	Fitness
Baseline	95.35%	95.19%	100%	95.51%
SPSO	**96.03%**	**96.26%**	**97.54%**	**96.17%**
FS	**96.05%**	**96.49%**	34.56%	93.18%
BE	95.67%	95.76%	87.05%	95.28%
GA	94.68%	95.21%	73.99%	93.90%
PSO	94.92%	95.27%	79.04%	94.16%
$\gamma = 0.1$ $(\alpha = \beta = 0.45)$				
Layout	SAI(RMSE)	SAI(M3S)	SAI(irregularity)	Fitness
Baseline	95.35%	95.19%	100%	95.74%
SPSO	**96.40%**	**96.69%**	**96.87%**	**96.58%**
FS	**95.97%**	**96.42%**	36.02%	90.18%
BE	95.46%	95.59%	89.92%	94.96%
GA	94.72%	94.94%	76.44%	92.99%
PSO	95.09%	95.41%	77.25%	93.45%
$\gamma = 0.15$ $(\alpha = \beta = 0.425)$				
Layout	SAI(RMSE)	SAI(M3S)	SAI(irregularity)	Fitness
Baseline	95.35%	95.19%	100%	95.98%
SPSO	**95.72%**	**96.06%**	**100%**	**96.51%**
FS	**95.57%**	**96.08%**	39.19%	87.33%
BE	95.26%	95.43%	91.59%	94.78%
GA	94.10%	94.31%	79.64%	92.02%
PSO	94.43%	94.86%	81.01%	92.60%
$\gamma = 0.2$ $(\alpha = \beta = 0.4)$				
Layout	SAI(RMSE)	SAI(M3S)	SAI(irregularity)	Fitness
Baseline	**95.35%**	95.19%	100%	96.22%
SPSO	**95.57%**	**95.94%**	**100%**	**96.60%**
FS	**95.66%**	**96.13%**	50.53%	86.82%
BE	95.26%	95.42%	91.81%	94.63%
GA	94.97%	95.18%	79.11%	91.88%
PSO	94.74%	95.13%	81.73%	92.30%

generate a marker layout at the same level as the irregularity of the baseline. In fact, the SAI(irregularity) values of the layouts of the algorithms other than SPSO were up to 91.81% in the experiments. In contrast, SPSO demonstrated reliability by creating a marker layout with comparable or even better irregularity than that of the baseline, as it was designed to iteratively search for the potential solution by taking into account the sparsity of the markers. From the experiments, we concluded that SPSO can substitute for the baseline with the advantages of improved overlay control, reliability and automatic generation.

IV. CONCLUSION AND DISCUSSION

In this paper, we proposed the SPSO algorithm, which can efficiently search a robust marker layout in a semiconductor photolithography process. We adopted a data-driven approach to evaluate the performance of potential solutions based on experiments and test data. The purpose of this approach is to avoid the risk of overfitting. However, the collected data from the semiconductor manufacturing process could generally not reflect all possible situations due to the dynamic nature of the process conditions; therefore, some outstanding solutions for the test data might not maintain their performance in an actual production stage. To overcome this problem, we suggested an irregularity measure to evaluate the possibility of whether a marker layout is overfitted to the collected data. In addition, the SPSO algorithm was designed to consider the locations of markers and maximize marker sparsity during the iterative solution generation process. During this process, the selection probability of markers is updated in an iteration-by-iteration fashion to prevent the markers from concentrating in specific areas, and the resulting marker layout can show better irregularity than other competitive layouts. In particular, if the ratio of irregularity had a large weight in the fitness function, the experimental results demonstrated that the SPSO layout outperformed the baseline layout in all measures.

This paper assumes that all fields of wafer have the same layout. However, it is possible to create a unique layout for each field or for each wafer area (e.g., wafer center and edge). It is commonly known from field experience that the overlay error is larger in the edge area than in the center area. To minimize the total overlay error of the wafer, the two searches (FS and BE) and SPSO will generate dense marker placement in the fields located at the edge area. In addition, the SPSO algorithm can be applied to search for the optimal marker layout when there are constraints on the locations of feasible markers. If some portion of a field is restricted from the allocation of markers due to preprocess or postprocess constraints, it is very burdensome to determine a marker layout using heuristics. In this case, the proposed algorithm can be a good alternative to investigate optimal marker layouts in any kind of marker array without further modification of the algorithm.

V. REFERENCES

[1] Y. Jiao and D. Djurdjanovic, "Stochastic control of multilayer overlay in lithography processes," *IEEE Trans. Semicond. Manuf.*, vol. 24, no. 3, pp. 404-417, Aug. 2011.

[2] C. F. Chien and C. Y. Hsu, "UNISON analysis to model and reduce step-and-scan overlay errors for semiconductor manufacturing," *J. Intell. Manuf.*, vol. 22, no. 3, pp. 399-412, Jun. 2011.

[3] B. Rangarajan, M. K. Templeton, L. Capodieci, R. Subramanian, and A. B. Scranton, "Optimal sampling strategies for sub-100-nm overlay," in *Proc. SPIE Metrol. Inspect. Process Control Microlithography XII*, Santa Clara, CA, United States, 1998, vol. 3332, pp. 348–360.

[4] C. F. Chien, K. H. Chang, and C. P. Chen, "Design of a sampling strategy for measuring and compensating for overlay errors in semiconductor manufacturing," *Int. J. Prod. Res.*, vol. 41, no. 11, pp. 2547-2561, 2003.

[5] C. F. Chue, T. B. Chiou, C. Y. Huang, A. C. Chen, and C. L. Shih, "Optimization of alignment/overlay sampling and marker layout to improve overlay performance for double patterning technology," in *Proc. SPIE Lithograhpy Asia*, Taipei, Taiwan, 2009, vol. 7520, pp. 1-12.

[6] N. L. Aung, W. J. Chung, L. Subramany, S. Hussain, P. Samudrala, H. Gao, X. Hao, Y. J. Chen, and J. M. Gomez, "Overlay Optimization for 1x node technology and beyond via Rule based Sparse Sampling," in *Proc. SPIE Metrol. Inspect. Process Control Microlithography XXX*, San Jose, CA, United States, 2016, vol. 9778, pp. 1-7.

[7] L. Subramany, W. J. Chung, P. Samudrala, H. Gao, N. Aung, J. M. Gomez, K. Gutjahr, D. S. Park, P. Snow, M. Garcia-Medina, L. Yap, O. N. Demirer, B. Pierson, and J. C. Robinson, "Advanced overlay: sampling and modeling for optimized run-to-run control," in *Proc. SPIE Metrol. Inspect. Process Control Microlithography XXX*, San Jose, CA, United States, 2016, vol. 9778, pp. 1-10.

[8] P. Wang, R. X. Gao, and R. Yan, "A deep learning-based approach to material removal rate prediction in polishing," *CIRP Annals*, vol. 66, no. 1, pp. 429-432, Apr. 2017.

[9] T. Jamrus, C. F. Chien, M. Gen, and K. Sethanan, "Hybrid particle swarm optimization combined with genetic operators for flexible job-shop scheduling under uncertain processing time for semiconductor manufacturing," *IEEE Trans. Semicond. Manuf.*, vol. 31, no. 1, pp. 32-41, Feb. 2018.

[10] R. Eberhart and J. Kennedy, "A new optimizer using particle swarm theory," in *Proc. 6th Int. Symp. Micro Mach. Human Sci.*, Nagoya, Japan, 1995, pp.39-43.

[11] J. Robinson and Y. Rahmat-Samii, "Particle swarm optimization in electromagnetics," *IEEE Trans. Anten. Propag.*, vol. 52, no. 2, pp. 397-407, Feb. 2004.

[12] R. Poli, J. Kennedy, and T. Blackwell, "Particle swarm optimization: An overview," *Swarm intell.*, vol. 1 no. 1, pp. 33-57, Jun. 2007.

[13] D. K. Agrafiotis and W. Cedeno, "Feature selection for structure-activity correlation using binary particle swarms," *J. Med. Chem.*, vol. 45, no. 5, pp.1098–1107, Feb. 2002.

[14] C. Y. Huang, C. F. Chue, A. H. Liu, W. B. Wu, C. L. Shih, T. B. Chiou, J. Lee, O. Chen, and A. Chen, "Using intrafield high-order correction to achieve overlay requirement beyond sub-40nm node," in *Proc. SPIE Metrol. Inspect. Process Control Microlithography XXIII*, San Jose, CA, United States, 2009, vol. 7272, pp. 1-9.

[15] W. C. Yeh and M. C. Chuang, "Using multi-objective genetic algorithm for partner selection in green supply chain problems," *Expert Syst. Appl.*, vol. 38, no.4, pp. 4244-4253, Apr. 2011.